On the road to ITER NBIs: SPIDER improvement after first operation and MITICA construction progress

V. Toigo[a], D. Marcuzzi[a], G. Serianni[a], M. Boldrin[a], G. Chitarin[a,b], S. Dal Bello[a], L. Grando[a], A. Luchetta[a], R. Pasqualotto[a], P. Zaccaria[a], L. Zanotto[a], R. Agnello[a,c], P. Agostinetti[a], M. Agostini[a], V. Antoni[a], D. Aprile[a,d], M. Barbisan[a,c], M. Battistella[a], G. Berton[a], M. Bigi[a], M. Brombin[a], V. Candeloro[a], A. Canton[a], R. Casagrande[a], C. Cavallini[a], R. Cavazzana[a], L. Cordaro[a], N. Cruz[a,e], M. Dalla Palma[a], M. Dan[a], A. De Lorenzi[a], R. Delogu[a], M. De Muri[a], S. Denizeau[a], M. Fadone[a], F. Fellin[a], A. Ferro[a], E. Gaio[a], F. Gasparini[a], C. Gasparrini[a], F. Gnesotto[a], P. Jain[a], P. Krastev[a,f], D. Lopez-Bruna[a,g], R. Lorenzini[a], A. Maistrello[a], G. Manduchi[a], S. Manfrin[a], N. Marconato[a], E. Martines[a], G. Martini[a], S. Martini[a], R. Milazzo[a], T. Patton[a], M. Pavei[a], S. Peruzzo[a], N. Pilan[a], A. Pimazzoni[a,d], C. Poggi[a], N. Pomaro[a], B. Pouradier-Duteil[a,c], M. Recchia[a], A. Rigoni-Garola[a], A. Rizzolo[a], E. Sartori[a,b], A. Shepherd[a,h], M. Siragusa[a], P. Sonato[a], A. Sottocornola[a], E. Spada[a], S. Spagnolo[a], M. Spolaore[a], C. Taliercio[a], D. Terranova[a], P. Tinti[a], P. Tomsič[a,i], L. Trevisan[a], M. Ugoletti[a], M. Valente[a], M. Vignando[a], R. Zagorski[a,l] A. Zamengo[a], B. Zaniol[a], M. Zaupa[a], M. Zuin[a], M. Cavenago[d], D. Boilson[m], C. Rotti[m], P. Veltri[m], H. Decamps[m], M. Dremel[m], J. Graceffa[m], F. Geli[m], M. Urbani[m], J. Zacks[m], T. Bonicelli[n], F. Paolucci[n], A. Garbuglia[n], G. Agarici[n], G. Gomez[n], D. Gutierrez[n], G. Kouzmenko[n], C. Labate[n], A. Masiello[n], G. Mico[n], J-F Moreno[n], V. Pilard[n], A. Rousseau[n], M. Simon[n], M. Kashiwagi[o], H. Tobari[o], K. Watanabe[o], T. Maejima[o], A. Kojima[o], E. Oshita[o], Y. Yamashita[o], S. Konno[o], M. Singh[p], A. Chakraborty[p], H. Patel[p,] N.P. Singh[p], U. Fantz[q], F. Bonomo[q], S. Cristofaro[q], B. Heinemann[q], W. Kraus[q], C. Wimmer[q], D. Wünderlich[q], G. Fubiani[r], K. Tsumori[s], G. Croci[t], G. Gorini[t], O. McCormack[a,t], A. Muraro[u], M. Rebai[u], M. Tardocchi[u], L. Giacomelli[u], D. Rigamonti[u], F. Taccogna[u], D. Bruno[u], M. Rutigliano[u], M. D'Arienzo[v], A. Tonti[w], F. Panin[z]

[a]Consorzio RFX (CNR, ENEA, INFN, UNIPD, Acciaierie Venete SpA), Corso Stati Uniti 4 – 35127 Padova, Italy
[b]Università degli Studi di Padova, Dept. of Management and Engineering, Strad. S. Nicola 3, 36100 Vicenza, Italy
[c]Ecole Polytechnique Fédérale de Lausanne (EPFL) - Swiss Plasma Center (SPC), 1015 Lausanne, Switzerland
[d]INFN-Laboratori Nazionali di Legnaro (LNL), v.le dell'Università 2, I-35020 Legnaro PD, Italy
[e]Instituto de Plasmas e Fusão Nuclear, Instituto Superior Técnico, Universidade de Lisboa, 1049-001 Lisboa, Portugal
[f]Institute for Nuclear Research and Nuclear Energy, Bulgarian Academy of Sciences, 72 Tsarigradsko Chaussee Boulevard, Sofia, 1784, Bulgaria
[g]Laboratorio Nacional de Fusión, CIEMAT, Madrid, Spain
[h]CCFE, Culham Science Centre, Abingdon, Oxon, OX14 3DB, UK
[i]University of Ljubljana, Faculty of Mechanical Engineering
[l]National Centre for Nuclear Research (NCBJ), PL-05-400 Otwock, Poland
[m]ITER Organization, Route de Vinon-sur-Verdon, CS 90 046, F-13067 St. Paul-lez-Durance, France
[n]Fusion for Energy,C/o Josep Pla 2, E-08019 Barcelona, Spain
[o]National Institutes for Quantum and Radiological Science and Technology (QST), 801-1 Mukoyama, Naka, Ibaraki-ken 311-0193, Japan
[p]ITER-India, Institute for Plasma Research, Nr. Indira Bridge, Bhat Village, Gandhinagar, Gujarat 382428, India
[q]IPP, Max-Planck-Institut für Plasmaphysik, Boltzmannstraße 2, D-85748, Garching bei München, Germany
[r]LAPLACE, Université de Toulouse, CNRS, Toulouse, France
[s]National Institute for Fusion Science, 322-6 Oroshi, Toki, Gifu 509-5292, Japan
[t]Dipartimento di Fisica "G. Occhialini", Università di Milano-Bicocca, Milano, Italy
[u]ISTP-CNR, Institute for Plasma Science and Technology, Via Roberto Cozzi 53 - 20125 Milano (MI), Italy
[v]ENEA, National Institute of Ionizing Radiation Metrology, C.R. Casaccia, S.Maria di Galeria, Italy
[w]INAIL-DIT, Via Ferruzzi, 40 - 00143 Roma
[z]INAIL-UOT Padova, Via Nancy, 2 - 35131 Padova

To reach fusion conditions and control the plasma configuration in ITER, the next step in tokamak fusion research, two neutral beam injectors (NBIs) will supply 16.5MW each, by neutralizing accelerated negative hydrogen or deuterium ions. The requirements of ITER NBIs (40A/1MeV D- ions for ≤1h, 46A/870keV H- ions for ≤1000s) have never been simultaneously attained. So in the Neutral Beam Test Facility (NBTF, Consorzio RFX, Italy) the operation

_____

corresponding author's email: gianluigi.serianni@igi.cnr.it

of the full-scale ITER NBI prototype (MITICA) will be tested and optimised up to full performances, focussing on accelerator (including voltage holding), beam optics, neutralisation, residual ion removal. The NBTF includes also the full-scale prototype of the ITER NBI source with 100keV particle energy (SPIDER), for early investigation of: negative ion production and extraction, source uniformity, negative ion current density and beam optics.

This paper will describe the main results of the first two years of SPIDER operation, devoted to characterizing plasma and beam parameters, including investigation of RF-plasma coupling efficiency and magnetic filter field effectiveness in reducing co-extracted electrons. SPIDER is progressing towards the first caesium injection, which aims at increasing the negative ion density. A major shutdown, planned for 2021, to solve the issues identified during the operation and to carry out programmed modifications, will be outlined.

The installation of each MITICA power supply and auxiliary system is completed; in-vessel mechanical components are under procurement by Fusion for Energy (F4E). Integration, commissioning and test of the power supplies, procured by F4E and QST, as the Japanese Domestic Agency (JADA), will be presented. In particular, 1.0MV insulating tests were carried out step-by-step and successfully completed. In 2020 integrated tests of the power supplies on the accelerator dummy load started, including the assessment of their resilience to accelerator grid breakdowns using a short-circuit device located in vacuum.

The aggressive programme, to validate the NBI design at NBTF and to meet ITER schedule (requiring NBIs in operation in 2032), will be outlined. Unfortunately, in 2020 the coronavirus disease infection affected the NBTF activities. A solution to proceed with integrated power tests despite the coronavirus is presented.

1. Introduction

The ITER experiment represents the next step in realising nuclear fusion as a viable energy source. To reach the fusion conditions and to control the plasma configuration in ITER, additional heating and current drive are provided by a combination of Neutral Beam Injectors (NBIs), Electron Cyclotron Resonance Heating and Ion Cyclotron Resonance Heating [1]. Two Heating NBIs will be installed to supply ITER with 16.5MW power each, with the possibility of a third injector, for a total of 50MW. The ion beam (hydrogen or deuterium) will be electrostatically accelerated up to 1MeV; at such beam energy, efficient (~60%) gas-cell neutralisation can only be achieved with negative ions. Negative ions are usually obtained by caesium-catalysed surface conversion of hydrogen/deuterium atoms in a plasma ion source. Satisfying the requirements of ITER NBIs (1MeV, 40A deuterium atoms, for one hour) is very challenging because such high performances have never been simultaneously attained. Therefore, in the dedicated ITER Neutral Beam Test Facility (NBTF) at Consorzio RFX (Italy) [2], the operation of the ITER NBI will be tested and optimised up to full performance. Experiments will verify the continuous operation of the NBI for one hour, including the stringent requirements on beam optics (divergence <7mrad, aiming within 2mrad). To study and optimise the performances of source and accelerator of the ITER NBI, the NBTF includes two test beds: MITICA, the full-scale ITER NBI prototype with 1MeV particle energy, and SPIDER, the full-scale prototype of the ITER NBI source, with an accelerator up to 100keV. SPIDER will profit from the experience gained at the ELISE test facility, at IPP-Garching (Germany), which aims at achieving the ITER requirements in a half size source, by developing ITER-relevant operation scenarios and by addressing specific aspects appearing during NBTF operation [3]. SPIDER will focus on the objectives, relevant for ITER, which are presently not addressed by ELISE, like beam extraction for 3600s as well as

validation of the electrostatic and magnetic configurations and of caesium distribution in an ITER-size source [4].

The main parameters of MITICA and ITER NBIs are given in Table 1. Table 2 displays the requirements for SPIDER: the extracted negative deuterium current density is defined as equal to the one required for ITER NBIs, considering that larger losses are expected inside the ITER NBI accelerator, which is much longer than the one in SPIDER. The SPIDER requirements in terms of negative hydrogen instead correspond to those required of ITER diagnostic neutral beam (60A negative hydrogen current accelerated to 100keV with an accelerator very similar to SPIDER [5]).

Table 1: Main MITICA parameters; the difference with ITER NBI is indicated.

Parameter	Value
Beam energy [keV]	1000 (D_2); 870 (H_2)
Max source filling pressure [Pa]	0.3
Max deviat. from uniform beam	±10%
Beamlet divergence [mrad]	≤ 7
Accelerated current [A]	40 D_2; 46 H_2
Beam on time	1 hour (H_2 in ITER: 1000s)
Co-extracted electron fraction	<1 in D_2; <0.5 in H_2

Table 2: Main SPIDER parameters.

Parameter	Value
Beam energy [keV]	100
Max source filling pressure [Pa]	0.3
Max deviat. from uniform beam	±10%
Extr. ion current density [A/m^2]	>355 H_2; >285 D_2
Beam on time	1 hour
Co-extracted electron fraction	<0.5 (H_2); <1 (D_2)

This paper gives an outline of the status of the ITER NBTF and of the activities carried out with SPIDER and in view of the start of MITICA operation. Finally the long-term planning of activities is sketched.

Few words are in order to remind that the coronavirus disease infection affected the efficiency of activities in 2020, resulting in a minor delay in SPIDER and MITICA activities.

2. SPIDER

As already mentioned, SPIDER represents the full-scale test-bed for the negative ion source of ITER NBIs [6]. Negative ions are generated in an inductively coupled plasma produced by 8 coils powered in pairs by 4 radiofrequency (RF) generators providing up to 200kW each. The plasma expands into a 0.8m wide and 1.8m tall chamber (expansion region), which is closed, opposite the drivers, by the plasma grid (PG), provided with 1280 apertures [7]. The apertures are arranged into 4×4 groups, each featuring 5(horizontally)×16(vertically) apertures, through which the negative ion beamlets are extracted, thanks to the electrostatic field induced by the voltage difference applied with respect to the next grid (extraction grid, EG); each grid is made of 4 segments, as described in [7]. Up to 100kV are then applied between the EG and the grounded grid (GG). Together with the negative ions, electrons are co-extracted from the plasma; a suitable arrangement of permanent magnets, embedded in the EG, dumps the electrons onto the EG itself; this field however deviates also the trajectories of negative ions, so that suitable countermeasures are needed to compensate for such negative ion deflection. The whole magnetic field configuration of SPIDER shares the basic principles with MITICA; in the case of SPIDER [8], the compensation of the negative ion deflection is performed by another system of permanent magnets embedded in the GG. Currents are run through the PG and dedicated other busbars to create a magnetic filter field just upstream with respect to the PG, to reduce temperature and density of electrons in the vicinity of the PG and to increase the plasma confinement inside the drivers, where most of neutral atoms, the precursors of negative ions, are generated.

During the last two years, as described in the next sections, SPIDER operation was devoted to steadily improving the availability of the system and to enlarging the range of the operational parameters for each plant. In this operational phase, without caesium injection, hydrogen and deuterium plasmas were characterised and the parameters of the negative hydrogen beam were investigated [9]. Several issues were identified during the experimentation [10], related to excessive gas pressure in the vessel, low RF-plasma coupling and sub-optimal magnetic filter field configuration; new and advanced diagnostics are providing first results or are under commissioning. Other experimental issues, requiring longer time to be solved, are being studied and the improvements will be implemented during a long shutdown planned for mid-2021 (see next sections); the most important ones will lead to enhancements of the beam source, of the vacuum system and of the RF generators. After the shutdown starting in 2021, it is planned that SPIDER experiments will resume without the presently known limitations, with operations aimed at reaching the expected nominal performances according to the general plan for the development of ITER NBIs.

2.1 Improvements of SPIDER in 2018-2020

The SPIDER beam source is in the same vacuum vessel as the one in which the beam propagates;

consequently, the vessel pressure is determined by the equilibrium between the gas inlet into the source and the pumping speed of the vacuum system. During the first SPIDER campaigns, a vessel pressure threshold was identified for the occurrence of RF discharges on the rear side of the source. Solving the issue requires enhancing the pumping system, as described in section 2.3. In the meantime, a temporary solution was quickly implemented to allow SPIDER operation, by installing a molybdenum mask on the downstream side of the PG [11], so that only 80 apertures out of 1280 were left open, thus limiting the gas flow out of the plasma source. Pulse durations in the order of several hundreds of seconds were allowed by subsequently substituting the material of the pushers, which keep the PG mask in position, from PEEK to DURAN 3.3® (PYREX) [12]. The thickness of the PG mask was also changed from 0.25mm to 0.64mm, to increase the PG mask stiffness with respect to out-of-plane deformation under heat load.
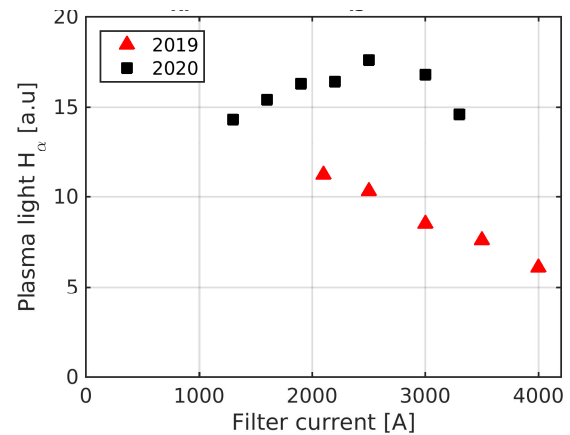

Fig. 1: plasma light (with H_α filter) along a line-of-sight through one of the RF drivers as a function of the filter field current, comparing the old and the new filter field configurations. Total RF power 360kW; source pressure 0.32Pa.

After an initial characterization of SPIDER plasma, experiments showed that, when increased above a certain threshold, the magnetic filter field severely impacted the plasma parameters, possibly resulting in complete quenching of the plasma. This effect was ascribed to the particular topology of the magnetic field inside the 8 inductively-coupled RF drivers that generate the plasma; dedicated experiments confirmed this assumption. Then a modified magnetic field configuration, closer to the configuration adopted in MITICA [13], was designed to reduce the plasma losses towards the driver surfaces, while keeping the magnetic field configuration almost unchanged in the region close to the PG, where the magnetic field profile was already as required [14]. The design of the new magnetic field configuration was based on numerical simulations of the current paths and on the assessment of the particle confinement in the drivers; to this purpose a test-particle trajectory code, both in 2D and 3D, including experimental profiles of the electric field in the driver, was applied. First experimental results show that the plasma quenching effect is no longer present with the new configuration: Fig. 1 shows that the H_α light emitted by the plasma inside the drivers is less affected by

the magnetic field than before, suggesting that now the plasma parameters are less sensitive to the filter field for intermediate values of the filter field itself: for usual filter field values in hydrogen (~2.5kA corresponding to 4mT in the vicinity of the plasma grid) the H_α light is a little higher than in the earlier configuration (this suggests a better plasma confinement inside the RF drivers) and it starts to decay for larger values of the filter field than before. While the plasma confinement inside the driver was improved, the non-uniformity between left and right drivers (which are connected in series to the same RF generator), appearing at high filter field, was confirmed, as discussed in the next section; it is worth noting that probe measurements inside the RF drivers showed that, in general, the variations of the H_α light corresponds to the behaviour of electron density (for electron temperature in the range 10-16eV and various values of gas pressure, RF power and filter field).

Also the power supplies were subjected to improvements arising from experimental needs [15]. The aforementioned RF-induced breakdowns on the rear side of the beam source generated over-voltages on the power supplies dedicated to polarising the PG and the bias plate, and also on the filament heating power supplies, with consequent intervention of protections and stop of the pulse. The issue was solved by optimising the electrical scheme of each power supply by adding parallel resistors. In caesium-free operation of negative ion sources, the required polarisation of the plasma grid with respect to the source walls can be larger than 30V in order to effectively reduce the amount of co-extracted electrons [16]; this voltage value exceeds the rating of the original SPIDER power supplies for plasma grid and bias plate. The issue was addressed by replacing the two power supplies with analogous devices, capable of providing up to 50V, but lower currents (200A), anyway compatible with most of present operations.

A set of three caesium ovens, not used in SPIDER yet, will evaporate caesium in the ion source, to improve the negative ion yield, particularly in the vicinity of the PG, where ion extraction occurs (dubbed extraction region). The caesium ovens for SPIDER will be installed on the rear wall of the ion source, remotely controlled and operated in vacuum up to temperatures of 350°C. A specific design was developed [17]; a prototype was tested and the caesium evaporation rate [18] of each oven as well as the caesium-specific diagnostics were characterised in a dedicated CAesium Test Stand (CATS) at the NBTF premises. As generation of negative ions relies on the proper distribution of caesium, good reliability is required of oven operation, which was demonstrated in steady state conditions along with the leak tightness of the sealing valve [19]. A final, on-site check is in progress regarding the noise immunity of the oven control circuitry. Just before the caesium campaign, the caesium ovens will be loaded with caesium and installed, ready for operation.

The cooling system is one of the most important plants of SPIDER, as the entire operation relies on removal of heat from the surfaces hit by the plasma (ion source) or by

the accelerated particles (accelerator grids, beam dump); moreover, most of the electrical power supplies are actively cooled. The heat rejection capacity required of SPIDER is 11MW. As high voltages are involved, the coolant fluid is ultra-pure water. The degradation of the coolant resistivity is being studied; it seems to occur preferentially inside the power supplies. The investigation is expected to result in devising strategies to prolong the lifetime of the cooling water [20].

An outline of the SPIDER diagnostic set is given in [21] (and references therein). Almost all diagnostic systems are operating, except those more specifically related to caesium operation, like Laser Absorption Spectroscopy and Cavity Ring-Down Spectroscopy. The latter was recently installed in SPIDER and aligned; preliminary tests during plasma pulses are ongoing [22]. A dedicated optical transmission module, to be operated in vacuum, was developed and installed for the front-end of the thermocouples located on the SPIDER grounded grid; the module provides tens of kV voltage insulation, to sustain the expected adverse effects of accelerator breakdowns. For specific purposes, new diagnostic systems have recently been realised or are under commissioning; two of them are described herein. Section 2.2 discusses an experimental campaign dedicated to the characterisation of generation and expansion of the plasma in SPIDER, from the RF drivers through the transverse magnetic filter. To this purpose a set of movable electrostatic probes was developed, entering the source plasma through the accelerator (plasma-only operation), thus minimising the perturbation of the measured quantities [23]. Several types of probes were installed in different positions and two configurations were adopted either to investigate the plasma in the RF drivers or in the expansion region. An Allison-type emittance scanner was developed to investigate the phase-space distribution of SPIDER beamlets [24]; this is a novelty in the field of power beam injectors and is motivated by the need of thoroughly investigating the beam features in view of the strict requirements for ITER NBIs. The device is composed of two slits on either side of a pair of parallel plates so that only particles entering with a specific inclination through the first slit can exit through the second one and be collected by a Faraday cup, after being deflected by the electric field inside the device. The emittance scanner, after tests in a dedicated facility, is being commissioned in SPIDER [25].

2.2 Plasma and beam operations in SPIDER

In the last two years SPIDER operation allowed to study different operational conditions and to characterise the plasma and the beam. Experiments were performed with hydrogen and with deuterium; caesium will be injected soon to increase the negative ion yield.

As mentioned, due to the presently limited pumping speed, a PG mask was introduced to allow operation at meaningful source pressure values (even >0.3Pa) without reaching gas pressure level inside the vessel that increases the risk of RF-induced discharges on the rear side of the source. Unlike other experiments, it was necessary to insert this PG mask on the downstream side of the PG, in

the 6mm gap between PG and EG. The molybdenum PG mask (the second version is 0.64mm thick instead of the earlier 0.25mm), is exposed to the plasma and is only weakly thermally connected to the PG, so that the mask temperature can rise during the plasma pulse well above the PG temperature itself. Thermal analyses and monitoring of the mask by an infrared camera, which was previously calibrated thanks to temporary thermocouples attached to the mask, allowed to trim pulse length and to prevent overheating of the fixing system (pyrex pushers, that keep the mask in position) due to thermal conduction from the mask itself. Experiments showed that around 400°C thermal radiation becomes effective in dissipating the heat and then the PG mask temperature stabilises with hydrogen; hence no specific pulse duration limits were identified with hydrogen. With deuterium, 400s pulses can be performed with respect to the pyrex operating temperature, provided that the magnetic filter field is strong enough to reduce the plasma density in front of the PG and thus the thermal load onto the PG mask.

A specific assessment of the operational constraints was carried out also on co-extracted electrons, which are deflected onto the extraction grid, where they deposit their kinetic energy; in the present operating conditions (no caesium), the contribution of negative ions to the extracted current is negligible. Electrons tend to focus when magnetically deflected, resulting in localised overheating. Numerical simulations of the particle trajectories can relate the spatial distribution of the impinging particles with their total associated power. Hence measuring the total electrical power fed by the EG power supply together with the numerical simulations of the particle trajectories, allowed the implementation of an interlock to stop SPIDER operation when the electrical power at the EG power supply exceeds 40kW, corresponding to 200°C locally, as per the simulations. This value for the interlock includes a conservative safety margin of a factor of 2, due to the local asymmetry of the electron energy flux with respect to the EG-average found in ELISE [16]. The numerical value of this interlock limit applies to the present condition, in which the amount of extracted particles is reduced by the PG mask.

Another limit on the beam power was defined and implemented to control the heat, mostly due to secondary electrons, impinging on the grounded grid, because the bottom segment is not actively cooled since the start of SPIDER operations, due to a leak identified at the end of assembly. This turns into a limit on the beam duration; direct measurement by thermocouple of the grounded grid temperature was adopted to verify the assumed amount of secondary particle in order to update the operational limit.

One of the most important aspects of SPIDER operation is the RF-plasma coupling, which has represented a major topic of investigation since the start of the experiments. The four SPIDER RF generators are self-oscillating power circuits (up to 200kW each) based on tetrodes. A first experimental finding was the criticality of operating the RF generators over their whole frequency range, since the interaction between oscillators, transmission line and ion source (which is a resonant

circuit in itself) makes the system unstable in the vicinity of the frequency match. As a consequence, and considering the magnetic coupling between the various generators on board the source, the maximum power at which the 4 RF generators can be simultaneously operated is ~100kW each [15]. Reaching this value of RF power per generator required the introduction of tuning, during the plasma pulse, of the self-oscillating frequency, regulated by the capacitors in the feedback chain of the tetrodes; the operational conditions are found to depend on the plasma, on the magnetic filter field and on the polarisation of plasma grid and bias plate. The RF generators produce noise at the RF frequency, which essentially disrupts the source thermocouple signals and heavily distorts the current-voltage characteristics of the electrostatic sensors; this issue is being addressed as discussed in section 2.3. To improve the control of the RF generators and to increase the RF power applied to the plasma, solid-state amplifiers are under consideration, also based on the ELISE experience [26]. Finally, comparison with source calorimetry has shown that the RF power measurement is inaccurate. These issues are being addressed, as described in section 2.3.
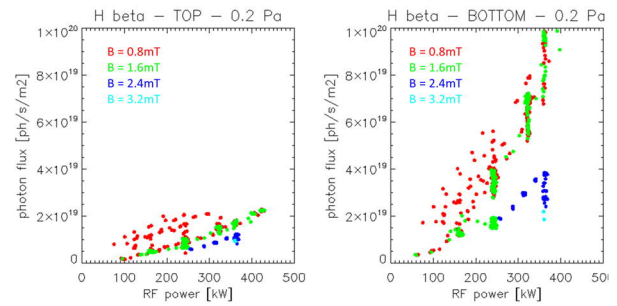

Fig. 2: brilliance of H_{beta} line as a function of the RF power with different values of the magnetic filter field: at the top of the plasma source (left) and at the bottom (right), close to the PG (extraction region); the source pressure is 0.23-0.27Pa.

Polarising the plasma grid normally allows to reduce the amount of co-extracted electrons [16]. Experimental time was devoted to investigating the influence of the polarisation of PG and bias plate on the currents of co-extracted electrons and on negative ions. The role of the plasma grid polarisation in reducing the co-extracted electrons is confirmed in SPIDER; the voltage applied to the bias plate can further enhance the reduction when it is slightly lower than the PG voltage.

Modelling the RF-plasma coupling gives also the possibility of estimating plasma parameters like the electron density inside the RF drivers. First results of this method are in line with measurements by electrostatic probes (see below) and are consistent with estimates from plasma spectroscopy [27].

Optical emission spectroscopy in the SPIDER source shows that the plasma fills the whole plasma chamber, despite the spatial localisation of the RF drivers. Vertical and horizontal profiles of the emitted light were measured, showing an increase of the brilliance with respect to the RF power and a decrease with the magnetic filter field (this is shown in Fig. 2 for

the horizontal lines-of-sight close to the plasma grid) [28]. It is also found that the extraction region seems more affected by the filter field than the driver region.

Between the end of 2019 and summer 2020, apart from the shutdown due to the coronavirus disease and to some commissioning of the cooling system, some weeks were devoted to the characterisation of SPIDER plasma with hydrogen and with deuterium [23]. Essentially two series of measurements were performed, one dedicated to the 3D characterisation of the expansion region and one devoted to the plasma in the RF drivers. Fig. 3 shows that the electron density increases with filling pressure, whereas the electron temperature decreases. In addition, for sufficiently high filter-field strength (4mT in the figure), a left/right asymmetry appears between the horizontal pair of drivers, which are connected to the same RF generator. The non-uniformity inside the RF drivers increases with pressure, in the range explored here (Fig. 3). During the same campaign, the measurements of the plasma parameters allowed also to estimate the drift motions inside the plasma.

The experimental measurements and particularly the asymmetries of the plasma parameters were investigated by means of a 2D-3V PIC-MCC simulation code written in C++/CUDA, which is under development to investigate the plasma expansion from the drivers towards the extraction region. The simulations preliminarily confirm the higher electron density towards the bottom of the source, induced by the plasma drift motions [29].
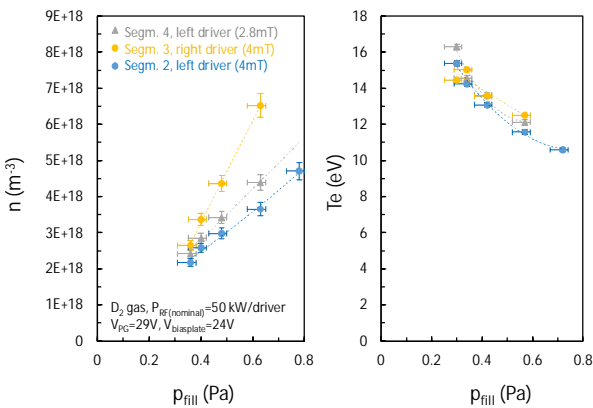

Fig. 3: Electron density (left) and temperature (right) as functions of the filling pressure in hydrogen in different vertical positions inside the expansion region; measurements from the first (top) segment are missing. The measurements at the bottom were collected with a lower value of the magnetic filter field at the PG.

The first beam operation in SPIDER showed that the electrical estimate of the negative ion current is about 2.5 times higher than the calorimetrical estimate obtained by the STRIKE calorimeter, since the former includes also secondary electrons [30]. Moreover, the beamlet divergence was estimated by several diagnostic systems; depending on the operational conditions, it reaches down to <20mrad. The SPIDER beam is investigated by different diagnostic systems, including visible cameras,

which are part of the beam tomography system [31]. After calibrating the cameras, application of inversion techniques allows to interpret the experimental data, providing information on the beam asymmetry; in the vertical direction, the asymmetry increases with magnetic filter field; in the horizontal direction it reproduces the left-right asymmetry observed in the driver plasma [28]. Beam operation in SPIDER was performed in hydrogen in two different periods; in the meantime, the magnetic filter field configuration and the plasma grid mask were changed. These modifications had no impact on the negative ion current, as shown in Fig. 4**Fehler! Verweisquelle konnte nicht gefunden werden.**; the small discrepancy can be attributed to a difference in the plasma grid and bias plate polarisations [32]: the ratio of co-extracted electrons to negative ions is around 55 in the former data set and 20 in the newer one, in which polarisation was employed, selectively reducing the electrons and slightly affecting the negative ions. It should also be mentioned that the stiffness of the new, thicker PG mask decreased the out-of-plane deformation of the mask itself, thus reducing the ellipticity (difference between the vertical and the horizontal sizes) of the beamlets.

In addition to what has already been mentioned, other numerical activities are carried out at the NBTF. A model for the simulation of the inductively-coupled plasma is being realized with 2D geometry and low frequency approximation for the conductivity; preliminary results confirm the non-negligible effect of the Faraday shield on the power coupled to the plasma. A suite of codes was applied in the past to design the accelerators of SPIDER [8] and MITICA [33]. A thorough comparison between codes and experiments is in progress, to verify the capabilities of the code to reproduce the experimental findings and to assess the extent to which reasonable additional physical hypotheses must be introduced [34].
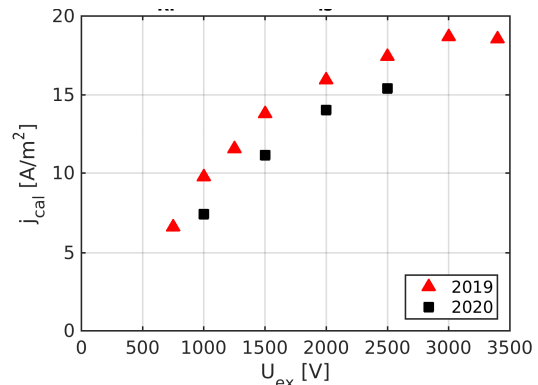

Fig. 4: Comparison of the negative hydrogen current density with the original configuration of the magnetic filter field and with the new one. In the old case, plasma grid and bias plate were floating; in the new one, they were current-controlled, emitting 100A; RF power 320kW; source pressure ~0.4Pa.

In summary, up to now, operation with SPIDER operation allowed to reach a negative ion current density up to $25A/m^2$, with a ratio of co-extracted electron current to negative ion current down to 15 and a minimum beamlet divergence of 16-20mrad depending on the diagnostic method; the operating conditions were: total

RF power up to 400kW, source pressure ~0.4Pa, filter field ~3mT, particle energy 27keV, large bias currents, no caesium injection.

2.3 Short-term planning for SPIDER

SPIDER operations will continue up to about mid-2021, when a major shutdown is scheduled to perform major modifications that cannot be realised in the short term or that require a long stop of the experiments. At the end of 2020, an improvement of the power supplies is planned. Specifically, the acceleration grid power supply is presently limited to 30kV as some components are not compliant with the European regulations. These components are being replaced. After the authorization will be issued and the software will be adapted, the acceleration grid power supply is expected to operate up to full performance. At the same time also the RF circuits are being improved: indeed, each RF circuit has a connection to the source potential on board the source; however the RF circuits are also connected to each other inside the high voltage deck by capacitive voltage dividers, which are necessary for the feedback control of the RF power and for the interlock on the RF voltage. To reduce the ensuing common-mode RF current, the voltage measurement is being moved before the internal transformer of the RF oscillator [35]. This modification will reduce the stray RF currents, which produced overheating the resistor of the output filter of the extraction grid power supply (this resistor was anyway replaced with one capable of dissipating up to 16kW) and induced RF noise on several diagnostic systems (high frequency filtering and common mode rejection was anyway implemented to protect some circuits) like the thermocouples.

A multi-year planning of SPIDER is given in section 4. The operation of SPIDER in the short term, from end of 2020 to early 2021 aims at assessing the suitability of SPIDER for caesium operation and at characterising the hydrogen and deuterium beam before caesium operation, including several minor tests that are almost completed (like the commissioning of caesium-related diagnostics). Afterwards, a short shutdown is planned to fill up the caesium evaporators. Then the source will be cleaned by long daily plasma-on time at high RF power and the caesium campaign with hydrogen will start, This will have the following goals:

- performing the caesiation of the source surfaces; this involves frequent and short pulses to distribute caesium with a 1/10÷1/6 duty cycle and a total of 2500s of plasma per day at relatively low RF power, with plasma grid possibly at 150°C and source walls at >35°C;
- characterising, when stationary conditions are reached, the negative ion beam with caesium operation; this requires short and frequent pulses with large RF power (100kW per generator);
- studying the resilience of the caesium layer during long pulses (up to 400s) at large RF power.

The beam characterisation pulses will involve scans of the different source parameters (filling pressure, RF power, filter field strength, polarisation of plasma grid and bias plate) and of the beam parameters (extraction and acceleration voltages), to qualify the beam optics, to maximise the negative ion current and to minimise the co-extracted electron current.

The cycle of the caesium operations will be repeated for increasing evaporation rates (at present, it is planned to use 5, 10, 20mg/h total caesium mass injection rates). The most promising one will represent the basis for the following experimental phase, with deuterium gas.

After this campaign with caesium, a major shutdown of the experiments is planned to carry out improvements and modifications, either planned since the beginning or emerged from the experimentation. The leaky segments of the grounded grid will be replaced; to this purpose, an analysis of the possible causes of the water leaks and of the corresponding remedial actions is in progress. During assembly of the accelerator, the magnets embedded in the grounded grid were installed with reversed polarity with respect to the design [10]. When the accelerator will be open, the magnets will be removed and re-installed correctly. In view of reducing the probability of RF-induced discharges on the rear side of the source, remedial actions include modifications to the topology of the RF drivers. Specifically, the following activities aim also at reducing the coupling among the RF circuits so as to extend the operational ranges of the plasma:

- geometry and material (alumina replaced by quartz) of the insulator lying beneath the RF coil, of the RF coils themselves (from Cu to AISI with 0.2mm electrodeposited copper) and of the separators of the coil windings (the so-called dolfin design) will be implemented; all of them will allow to keep a gap between coil and case of 2mm; improvement to surfaces and edges will be kept into account wherever possible;

- the RF circuit connections will be optimised in terms of loop area reduction, electrical contact quality and minimisation of extension for high current/voltage links;

- the possibility of changing the coil pairing and layout will be implemented.

As already mentioned, also the SPIDER vacuum system has to be enhanced during the major shutdown in order to reduce the probability of RF-induced discharges. The throughput of hydrogen with beam source operated at 0.3-0.6 Pa was calculated. Correspondingly, given the measured conductance of the source, the additional pumping speeds to be installed were estimated 100-300m^3/s, respectively, to be compared with the present nominal 100m^3/s. Increasing the performances of the vacuum system may in principle be undertaken with commercial cryogenic pumps, like the ones currently installed, but would require a non-manageably large additional quantity of pumps. Remaining options are customised cryogenic panels fed by a dedicated cryogenic plant or Non-Evaporable Getter pumps (NEG) [36]. Both options are under considerations and pros and cons have been assessed [37]; further investigations on both solutions shall soon allow to converge on the most promising proposal. At the moment NEG pumps, which

require completion of definitive demonstration for suitability, seem to be capable of more strategic flexibility at a lower impact and likely at a lower overall price.

In view of the removal of the SPIDER beam source from the vessel, other activities are in progress, like the preparation of a system devoted to draining and drying the in-vessel actively cooled components of SPIDER. The drying system is designed to limit as much as possible atmospheric corrosion inside the hydraulic circuits and components, to prevent water spreading, and to allow the execution of vacuum leak tests of the hydraulic circuits before re-installation inside the vacuum vessel [38]. Draining will be first performed by gravity after opening the end connections of hydraulic circuits and then by blowing the water out by inert gas. Injection of pressurized nitrogen is simulated by means of one-dimensional and three-dimensional models to perform transient two-phase analyses in order to calculate the minimum required inlet pressure and to estimate the process time [39].

3. Status of MITICA

The MITICA facility is the full-scale prototype of the entire Heating Neutral Beam injectors (HNBs) for ITER. MITICA, like SPIDER, will continue operating in parallel and in support to the HNBs and for improving the HNBs.

The installation and commissioning of mechanical components and plants of MITICA continued fairly regularly, in particular the vessel, the cooling plant, the gas and vacuum system, and the cryogenic plant. Only the in-vessel components, such as the ion source/accelerator, the beam line components and the cryogenic pumps, are still under construction.
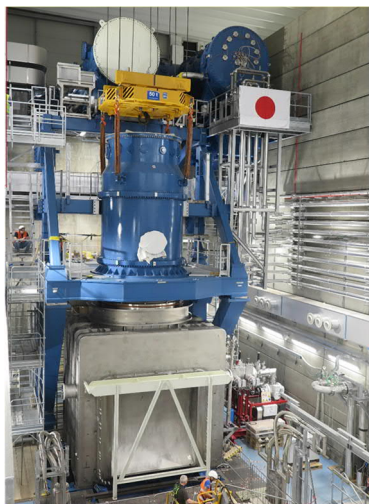

Fig. 5: Lowering, positioning and fixing of HV bushing to support structure and BS vessel.

The power supply systems feeding the accelerator and the ion source have been completed. In particular, the 1MV transmission line from the 1MV generator was connected to the vacuum vessel through the High Voltage (HV) bushing which acts as a barrier between the transmission line, insulated by SF_6 gas at 6bar, and the vacuum present in the vacuum vessel.

Fig. 5 shows the HV bushing being lowered over the beam source (BS) vessel during its installation.

The installation of the other auxiliary systems necessary for the operation of MITICA have also been completed, such as the cooling system, the vacuum and gas injection system and the cryogenic system for the cryogenic pumps. The commissioning activities are well advanced and by the end of 2020 they will be mostly ready for operation.

The vacuum vessel [40], composed of two parts, Beam Source Vessel (BSV) and Beam-Line Vessel (BLV), see Fig. 6, was completed. In particular, the latter was installed and tested at the beginning of 2020 just before the on-site activities were interrupted for about 2 months due to the coronavirus disease infection.

Fig. 6: View of the BLV installed inside MITICA bunker. The leak test of BSV+BLV (part of the SAT) was completed before the coronavirus lockdown.

The integrated commissioning and the power tests of the power supplies have already begun; they are planned to end in 2021, when the facility will be prepared and used to carry out HV holding tests in vacuum by utilizing electrostatic mock-ups instead of the beam source, as shown in Fig. 13.

The in-vessel mechanical components are still in the procurement phase by F4E. They will be delivered and installed between 2022 and 2023. The experimental activity without acceleration will begin at the beginning of 2023. Subsequently, at the beginning of 2024, after the installation of the Beam-Line Components (BLCs) it will be possible to extract the beam and to accelerate it to high energy.

3.1 Power supply integration and power tests

The MITICA power supply is a very complex system, including power conversion systems, HV components, insulated by air or SF_6 gas, controls and interlocks. The procurement of the MITICA power supply is shared between F4E and QST as the JADA; as a consequence, also the integration process is very complex, since it must also take into account the different responsibilities.

After installation completion [41], a long integrated commissioning process started in 2018 with the first

insulation tests up to 1.2MVdc. The insulation tests were carried out in subsequent steps, to verify the various parts while they were gradually added to the system. The tests lasted until 2019 when, with the connection of the transmission line to the vacuum vessel through the HV bushing, it was possible to verify the complete system. In parallel, the power supply system of the ion source, housed inside a large (12.5m (L) x 8.4m (W) x 9.6m (H)) -1MVdc air-insulated Faraday cage, called HVD1, was also installed and commissioned, and is now ready to be connected to the beam source.

In Fig. 7 a view is shown of the HVD1 hosting the ion source power supply and the HV Bushing of the 1MV insulating transformer feeding the Ion Source and Extraction Power Supplies (ISEPS). The scaffolding for the access inside the HVD can be noticed; this must be removed before applying high voltage.

Fig. 7: View of the HVD1 hosting the ion source power supplies and the HV bushing of the 1MV insulating transformer feeding the ISEPS.

Integrated power tests require a 1MV dummy load capable of dissipating the full power, 50MW, for a couple of seconds. It consists of a system of natural air-cooled resistors that can be reconfigured to perform tests even at reduced power levels. The tests also include the simulation of the breakdowns between the acceleration grids. This is simulated by a system of spark gaps installed inside the vessel instead of the source and pneumatically controlled from the outside. The insulation of the spark gaps is obtained by filling the vessel with SF_6 gas at a pressure slightly higher than the atmosphere (1.3bar).

Fig. 8: AGPS 1MV, 50MW resistive dummy load

At the conclusion of the insulation tests, the dummy load was installed beside the HVD hall, see Fig. 8, and the short-circuiting device was positioned inside the BS vessel, see Fig. 9. In addition, other arrangements have been made to ensure the proper functioning of the power supply system, such as the installation of ringing filters between converters and step-up transformers to avoid over-voltages on the transformer windings during the switching of the inverters [42].

The restrictions due to coronavirus call for a new organization model for the integration tests of the power supplies provided by the Japanese and European partners. This organization is based on the presence of a supervisor nominated directly by JADA on site who communicates in real time with the QST experts and the company that manufactured the systems in Japan. A multichannel communication net was set up providing real-time data during testing to allow a shared monitoring of plant performance and integration capability, and at the same time collecting feedback from the personnel in Japan.

This organization was set up and tested in September 2020, during the test preparation activities. Subsequently, the first integration tests were carried out by operating the individual stages of the accelerator, which is composed of 5 stages connected in series (designed to operate at 200kV each) at reduced voltage and power to verify the correct operation of the control and regulation systems. The organization worked properly and also this test was successfully completed. In Fig. 10 the first waveforms of voltage and current produced at the output of the AGPS power supply are displayed. The generated voltage was limited to only 50kV for safety reasons (it was operated without the insulation gas to facilitate accessibility inside the components in case of inspection).
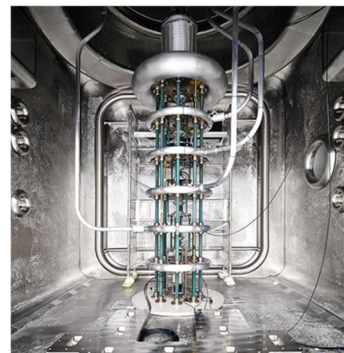

Fig. 9: Short-circuiting device inside BSV to simulate the grid breakdowns during the AGPS power integrated tests

These tests will continue at no-load conditions up to 1MV. They are expected to start by the end of 2020 and to be completed in early 2021.

3.2 In-vessel mechanical components

The remaining procurements featuring in-vessel components, i.e. beam source and accelerator, beam line components and cryogenic pumps, are still in the factory

phase. Most of the activities have progressed and are ongoing although with some limitations, both on the supplier side and on the customer follow-up side. Update of each delivery date on site is being accounted for in the revised overall schedule and is monitored carefully.

In particular, beam line components procurement has entered the engineering phase of the manufacturing, with process qualification and construction of prototypes for various parts (Fig. 11), while the Beam Source is between the end of the engineering phase and the beginning of the production of most parts, with prototypes under completion by several sub-suppliers (Fig. 12).
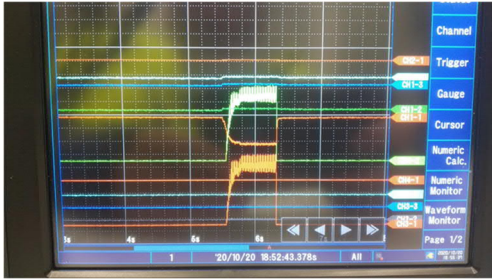
Fig. 10: Voltage and current waveforms generated in the output of one stage of the MITICA AGPS.
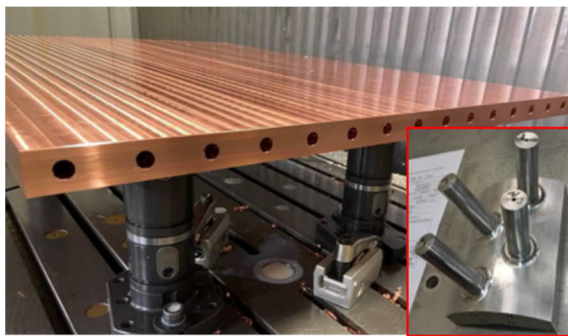
Fig. 11: Prototypes for qualification of deep drilling for ERID panel and extrusion/welding for Calorimeter manifolds
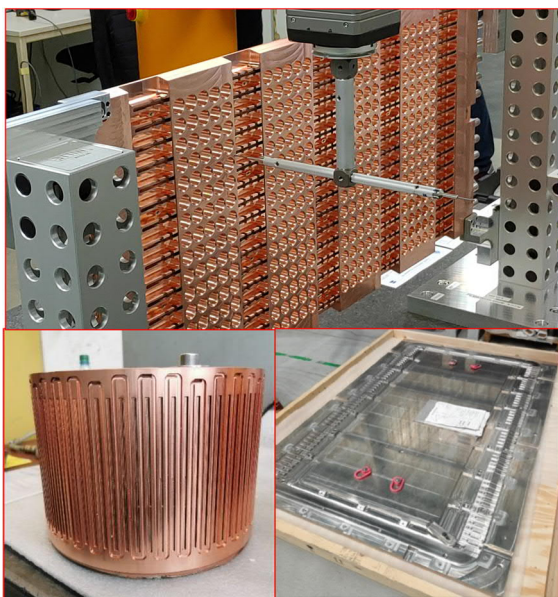

Fig. 12: Prototyping in view of MITICA: AG4 prototype completed (on top) and intermediate phase for manufacturing of

Faraday shield (bottom left) and series-produced parts for the support plates (bottom right).

3.3 High voltage holding tests in vacuum

HV test campaigns in vacuum on MITICA test bed, planned to start in 2021 before the installation of in-vessel components, shall allow to gain insights into one of the main topics to be investigated in MITICA. The main objectives of the test strategy have been identified:

- to verify and improve the insulation of MITICA up to 1MV in vacuum as well as with low pressure gas, before the installation of the beam source;

- to establish and validate voltage holding scaling laws for large gaps and multiple electrodes.

A specific project was launched for the design, procurement and installation of a set of Mock-up Electrodes (ME) and Electrostatic Shields (ES) replicating MITICA BS geometries to be interfaced with High Voltage Bushing (HVB) and Beam Source Vessel, hence exploiting the time window before the delivery of the actual source for the execution of these tests.
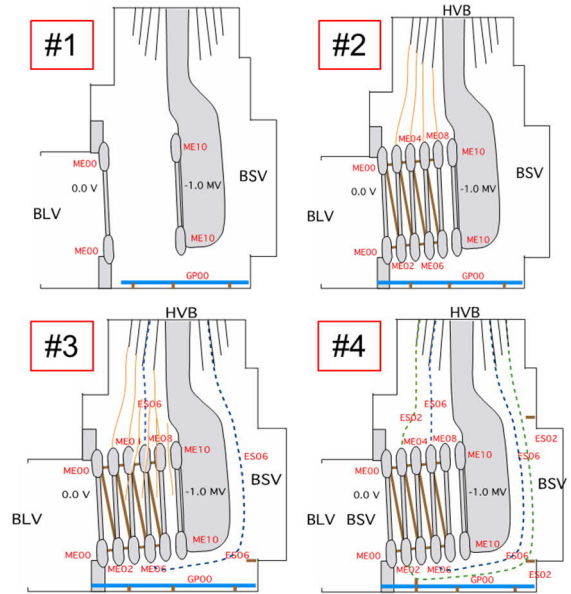

Fig. 13: Staged approach for HV tests in vacuum.

A staged approach has been set, corresponding to the configurations (shown in Fig. 13) to be progressively tested towards the thorough assessment and the final goal. The first configuration includes just the mock-up representing the outer shape of parts at ground potential and at -1 MV; the second one encompasses also the outer elements of the intermediate electrodes composing MITICA accelerator, and the following configurations feature the additional intermediate shields, which would envelop the rear side of the source to further increase the voltage holding.

In addition, the following ancillary elements have been identified and added to the test configuration: vacuum pumping system, monitoring cameras and electrical measurement systems.

4 Long-term planning of the NBTF

ITER multi-year planning is described in [43]. The Heating NBIs (HNBs) will be operating to heat the ITER plasma during the Pre-Fusion Power Operation-II, due to start in June 2032. This milestone and the ensuing requirements on procurement of beam source and beam-line components for the ITER NBIs, define the overall plan of SPIDER and MITICA (Fig. 14), which also depends on the delivery dates of the in-vessel MITICA components to be supplied by F4E. The schedules of SPIDER and MITICA are linked together, as the start of the operational phase of the MITICA ion source will profit from the results of the SPIDER operations.

In general, the experiences gained during SPIDER experiments are functional to speeding up MITICA operations and tuning up to the full performances, whose planning in turn is strictly linked to the ITER HNBs. Specifically, SPIDER will be operated in the present conditions up to the 2021 shutdown, in order to complete the first investigations of the source and of a reduced-size beam. While the MITICA beam source will be under installation, SPIDER operations will be devoted to verifying the plasma initiation in view of the start of the MITICA ion source, at medium RF power, and without caesium. In the meantime, the SPIDER beam will be optimised at medium RF power and experience on long pulses will be gained. Thus, after the installation of MITICA beamline components, SPIDER will provide indications for the first beam operation in MITICA, without and, subsequently, with caesium. At that time, SPIDER might undergo a major shutdown to improve it in view of high beam power and long pulse operations, while the outcome of MITICA activities will be transferred to the final HNB design. The modifications tested in SPIDER might be inserted in MITICA, for validation during the extended MITICA operation, in view of the HNB operation and also in view of possible re-fabrication of HNB grids for a second generation, if necessary.
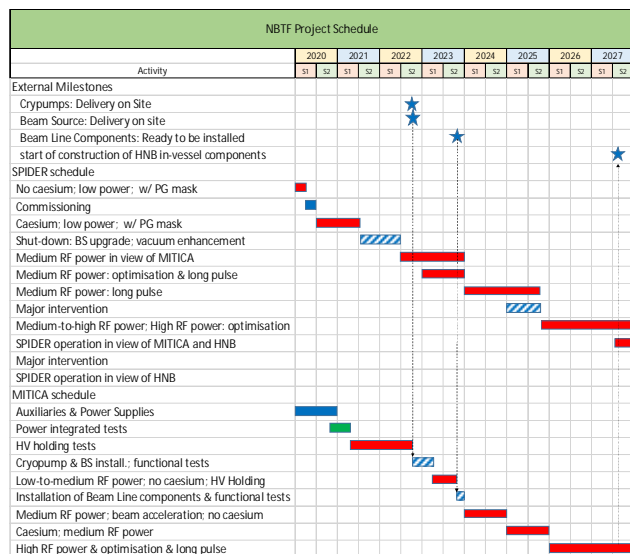

Fig. 14: Multi-year project schedule of the NBTF.

5 Summary

The present paper gives an overview of the status of the test facility for ITER neutral beam injectors. Two devices are operated: the full-scale test stand of the negative ion source, SPIDER, is operating since June 2018 and has already provided data about hydrogen and deuterium plasmas as well as about hydrogen beam. During the experiments several issues emerged, which were mostly solved, leading to a global improvement of the ion source. The present SPIDER operations aim at injecting caesium inside the ion source to increase the negative ion yield; this is planned for early 2021. The full-scale test stand of the entire injector, MITICA, is under completion. High voltage tests are planned for the next years and plasma experiments will start as soon as the ion source will be delivered and installed. Afterwards, beam operations will be conducted, according to a global plan, which is tightly linked with the overall ITER schedule.

References

[1] D. Campbell, Phys. Plasmas **22** (2015) 021701
[2] V. Toigo et al., New J. Phys. **19** (2017) 085004
[3] U. Fantz et al., Fusion Eng. Des. **156** (2020) 111609
[4] V. Toigo et al., Nucl. Fusion 59 (2019) 086058
[5] A. Chakraborty et al., IEEE Trans. Plasma Sci., **38** (2010) 248
[6] P. Sonato et al., Fusion Eng. Des. **84** (2009) 269
[7] D. Marcuzzi et al. Fusion Eng. Des. **85** (2010) 1792
[8] P. Agostinetti et al., Nucl. Fusion **51** (2011) 063004
[9] G. Serianni et al., Rev. Sci. Instrum. **91** (2020) 023510
[10] G. Serianni et al., Fusion Eng. Des. **146** (2019) 2539
[11] M. Pavei et al., Fusion Eng. Des. **161** (2020) 112036
[12] M. Pavei et al., Improvements to SPIDER beam source after two years of operation, this conference
[13] N. Marconato et al., Fusion Eng. Des. **96-97** (2015) 517
[14] N. Marconato et al., Fusion Eng. Des. **166** (2021) 112281
[15] A Zamengo et al., Power Supply system for large Negative Ion Sources: early operation experience on the SPIDER experiment, submitted to IEEE Trans. Plasma Sci.
[16] P. Franzen et al., Plasma Phys. Control. Fusion **56** (2014) 025007
[17] A. Rizzolo et al., Fusion Eng. Des. **88** (2013) 1007
[18] E. Sartori, IEEE Trans. Instrum. Meas. **69** (2020) 4975
[19] M. De Muri et al., Fusion Eng. Des. **167** (2021) 112331
[20] C. Cavallini et al., Fusion Eng. Des. **166** (2021) 112271
[21] R. Pasqualotto, J. Instrum. **12** (2017) C10009

[22] M. Barbisan et al., Development and first operation of a Cavity Ring Down Spectroscopy diagnostic in the negative ion source SPIDER, accepted for publication in Rev. Sci. Instrum.

[23] E. Sartori et al., Fusion Eng. Des. **169** (2021) 112424

[24] C. Poggi et al., Rev. Sci. Instrum. **91** (2020) 013328

[25] C. Poggi et al., First tests and commissioning of the emittance scanner for SPIDER, under revision for publication in Fusion Eng. Des.

[26] B. Heinemann et al., Fusion Eng. Des. **136** (2018) 569

[27] P. Jain et al., Estimation of electron density inside a radio frequency inductively coupled driver of SPIDER, TA3-S1-050 - Oral presentation - 47th IEEE International Conference on Plasma Science, ICOPS 2020, December 6th- 10th, Singapore

[28] B. Zaniol et al., Rev. Sci. Instrum. **91** (2020) 013103

[29] V. Candeloro, Modelling of plasma expansion and interpretation of measured profiles in a negative ion source, Master thesis in Physics, Padova University, (2020)

[30] A. Pimazzoni et al., Rev. Sci. Instrum. **91** (2020) 033301

[31] M. Ugoletti et al., Characterization of SPIDER beam emission profile through beam imaging, under revision for publication in Fusion Eng. Des.

[32] A. Pimazzoni et al., Fusion Eng. Des. **168** (2021) 112440

[33] P. Agostinetti et al., Nucl. Fusion **56** (2016) 016015

[34] S. Denizeau et al., Fusion Eng. Des. **168** (2021) 112374

[35] A. Maistrello et al., Fusion Eng. Des. **167** (2021) 112337

[36] M. Siragusa et al., Rev. Sci. Instrum. **91** (2020) 023501

[37] S. Dal Bello et al., Improvement of SPIDER vacuum system, presented at 31 SOFT conference

[38] F. Fellin et al., Design and procurement of the Drying System for SPIDER Beam Source, under revision for publication in Fusion Eng. Des.

[39] M. Zaupa et al., Fusion Eng. Des. **170** (2021) 112531

[40] M. Valente, Fusion Eng. Des. **169** (2021) 112473

[41] M. Boldrin et al.; Fusion Eng. Des. **164** (2021) 112170

[42] M. Dan et al., Design and test of a mitigation system against voltage ringing in MITICA AGPS, under revision for publication in Fusion Eng. Des.

[43] B. Bigot, Nucl. Fusion **59** (2019) 112001